Alma Mater Studiorum Università di Bologna
Archivio istituzionale della ricerca

Photoinduced Electron Transfer Involving a Naphthalimide Chromophore in Switchable and Flexible [2]Rotaxanes

(Article begins on next page)

20 April 2024

Photoinduced Electron Transfer Involving a Naphthalimide Chromophore in Switchable and Flexible [2]Rotaxanes

Benoit Colasson,*[a],[b] Alberto Credi*,[c],[d],[e] and Barbara Ventura*[e]

Dedicated to Jean-Pierre Sauvage on his 75th birthday

Abstract: The interlocking of ring and axle molecular components in rotaxanes provides a way to combine chromophoric, electron-donor and electron-acceptor moieties in the same molecular entity, in order to reproduce the features of photosynthetic reaction centers. To this aim, the photoinduced electron transfer processes involving a 1,8-naphthalimide chromophore embedded in several rotaxane-based dyads were investigated by steady-state and time-resolved absorption and luminescence spectroscopic experiments in the 300 fs-10 ns time window. Different rotaxanes built around the dialkylammonium / dibenzo[24]crown-8 ether supramolecular motif were designed and synthesized to decipher the relevance of key structural factors, such as the chemical deactivation of the ammonium-crown ether recognition, the presence of a secondary site for the ring along the axle, and the covalent functionalization of the macrocycle with a phenothiazine electron donor. Indeed, the conformational freedom of these compounds gives rise to a rich dynamic behavior induced by light, and may provide opportunities for investigating and understanding phenomena that take place in complex (bio)molecular architectures.

Introduction

Photoinduced electron transfer (PET) is one of the key processes that occur during the photosynthesis. It takes place in the photosynthetic reaction center (RC), in which the optimized organization of the donor-acceptor (D-A) pairs enables a directional electron migration and eventually leads to a long-lived charge separation.[1] Remarkably, the transfer of charge between the various D and A units follows a non-covalent pathway that allows for the optimization of the thermodynamic and kinetic coupling, and a structural reorganization after the electron transfer events.[2] In the frame of research on artificial photosynthesis, both covalently linked and self-assembled multicomponent RC model systems have been investigated. The former have the advantage of a precise relative positioning of the subunits, but are often synthetically challenging and the lack of flexibility can limit their performance. The latter, on the other hand, are stable under specific experimental conditions that do not necessarily coincide with those optimal for photoinduced charge separation.

An interesting possibility to combine D and A units in a molecular species with the aim to reproduce the features of natural RCs is to exploit the mechanical bond in interlocked molecular architectures such as rotaxanes.[3] Minimally, a rotaxane consists of a molecular ring that encircles a molecular axle stoppered at both extremities such that a mechanical link is established between the components. When the D-A pair is installed in the rotaxane in such a way that D (or A) is attached to the ring and A (or D) is on the axle, the mechanical bond guarantees enough flexibility to enable many conformations of the dyad (i.e. mutual D-A arrangements), while not only preventing the dissociation of the components but also limiting their degree of freedom in the three directions of space. In addition, providing that the interaction between the ring and the axle can be modulated by an external stimulus, the conformation of the dyad can be modified accordingly. Different D-A pairs embedded in a rotaxane were synthesized and studied as models of the photosynthetic center in the context of artificial photosynthesis.[4] For instance, Sauvage and co-workers reported on multiporphyrinic rotaxanes.[5-7] C_{60} has also been exploited for its photophysical and redox properties as an electron acceptor in rotaxanes developed by Sauvage et al.,[8] Ito at al.[9] and Schuster, Guldi, et al.[10-12] Although the high flexibility of such large systems often prevents a clear interpretation of the results, these studies highlight the importance of the mutual arrangement between the chromophores in the efficiency of the PET process.

In principle, a better control of the distance is expected when D and A are incorporated in the ring and axle components of a bistable molecular shuttle, i.e. a rotaxane that has two different macrocycle recognition sites (stations) on the axle (Figure 1). For instance, a fine tuning of the electron-transfer kinetics was demonstrated in a C_{60}-ferrocene rotaxane in which the distance between A and D is dictated by the polarity of the solvent.[13] Nevertheless, our recent studies on bistable rotaxanes based on

[a] Dr. B. Colasson, Université de Paris, UMR 8601, LCBPT, CNRS, 45 rue des Saints-Pères, F-75006 Paris, France.
E-mail : benoit.colasson@parisdescartes.fr
[b] Dr. B. Colasson, Photochemical Nanosciences Laboratory, Dipartimento di Chimica "G. Ciamician", Università di Bologna, via Selmi 2, 40126 Bologna, Italy.
[c] Prof. A. Credi, Dipartimento di Scienze e Tecnologie Agro-alimentari, Università di Bologna, viale Fanin 50, 40127 Bologna, Italy.
E-mail: alberto.credi@unibo.it
[d] Prof. A. Credi, CLAN – Center for Light Activated Nanostructures, Università di Bologna and Consiglio Nazionale delle Ricerche, via P. Gobetti 101, 40129 Bologna, Italy.
[e] Prof. A. Credi, Dr. B. Ventura, Istituto ISOF-CNR, via P. Gobetti 101, 40129 Bologna, Italy.
E-mail: barbara.ventura@isof.cnr.it

Supporting information for this article is given via a link at the end of the document.

ammonium and viologen stations[14] unraveled details on the effective control on the distance when a flexible macrocycle such as dibenzo[24]crown-8 (DB24C8) is part of the structure.[15] In particular, by incorporating spin-labels on the DB24C8 ring and at one stopper extremity of the thread, a combination of electron-electron double resonance spectroscopy and molecular dynamics calculations indicated that the stimuli-induced shuttling of the ring along the axle is accompanied by a large conformational rearrangement of the ring, eventually leading to a limited modification of the distance between the two spin-labels.
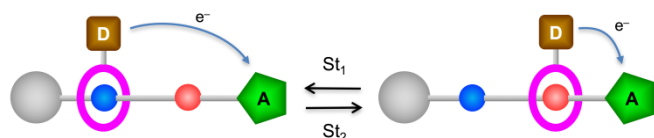
Figure 1. The stimuli-induced ring shuttling between two stations along the axle in a bistable rotaxane can be used to modulate the efficiency of distance-dependent processes such as electron transfer.

More specifically, the DB24C8 ring can exist in two extreme conformations: (i) a V-shaped form in which the two aromatic units are folded on the same side of the macrocycle, and (ii) a Z-shaped form in which the two catechol rings are anti-parallel (see Scheme 1; the conformational changes were transposed to the rotaxanes studied in this work, *vide infra*). These two conformations were previously observed in the X-ray crystal structure of rotaxane-type compounds containing the DB24C8 ring.[16-18] In the context of electron transfer, the main consequence of this rearrangement (not to mention the flexibility of the axle) is that the triggered translational motion of the ring does not guarantee the operator to have a perfect control over the distance change between A and D. Here we report on an in-depth study aiming at deciphering the influence of the flexibility and relative arrangement of the molecular parts on the photophysical properties of an acid-base switchable rotaxane designed to behave as a dyad for photoinduced electron transfer. Moreover, we explore the role of the bare DB24C8 macrocycle – a highly popular ring for mechanically interlocked molecules[3] – in photoinduced electron transfer processes that occur between the interlocked ring and axle components.
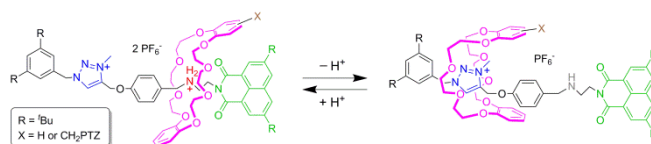

Scheme 1. The acid-base triggered rearrangement of the rotaxanes studied in this work. Two selected conformations for the flexible ring are represented to emphasize the fact that shuttling does not necessarily result in a net modification of the distance between A (naphthalimide stopper) and D [phenothiazine (PTZ) unit appended to the DB24C8 macrocycle]. Other ring conformations and relative ring-axle orientations are possible for both states.

Results and Discussion

Design and synthesis

Rotaxanes based on a DB24C8 macrocycle surrounding an axle composed of a dialkyl-ammonium (amH$^+$) and a triazolium (tria$^+$) stations have recently been proposed as acid-base switchable molecular devices.[19-30] These rotaxanes can be readily synthesized and easily functionalized either at the ring or at the axle. Hence, we designed a [2]rotaxane bearing a phenothiazine (PTZ) donor unit linked to the crown ether ring and a photoactivable naphthalimide (NI) acceptor unit as a stopper (Scheme 1). These two groups have been previously associated in several D-bridge-A-type dyads in which the photo-induced charge separated state NI$^{•-}$−PTZ$^{•+}$ was observed.[31-36] In the protonated state of the rotaxane, the ring encircles the amH$^+$ station and interacts with it *via* hydrogen bonds. After deprotonation, the affinity of the ring for this station vanishes and the ring translates and resides on the tria$^+$ station. Protonation of the amine resets the system back to its initial situation (Scheme 1). This operation should in principle modify the spatial arrangement between A and D and, as a consequence, tune the PET characteristics of the dyad.

The rotaxane dyads, the molecular components and the model compounds considered in this study are represented in Figure 2. Rotaxanes with two stations (amH$^+$ and tria$^+$), in which the ring surrounds the amH$^+$ site, are denoted as **2s**; the corresponding deprotonated species, wherein the ring is located on the remaining tria$^+$ station, are identified with a prime. Rotaxanes labelled **1s** possess only the amH$^+$ station (the tria$^+$ station is lacking because the triazole unit is not methylated). The representation of the DB24C8 macrocycle in Figure 2 has no implication regarding its conformation in the rotaxanes.
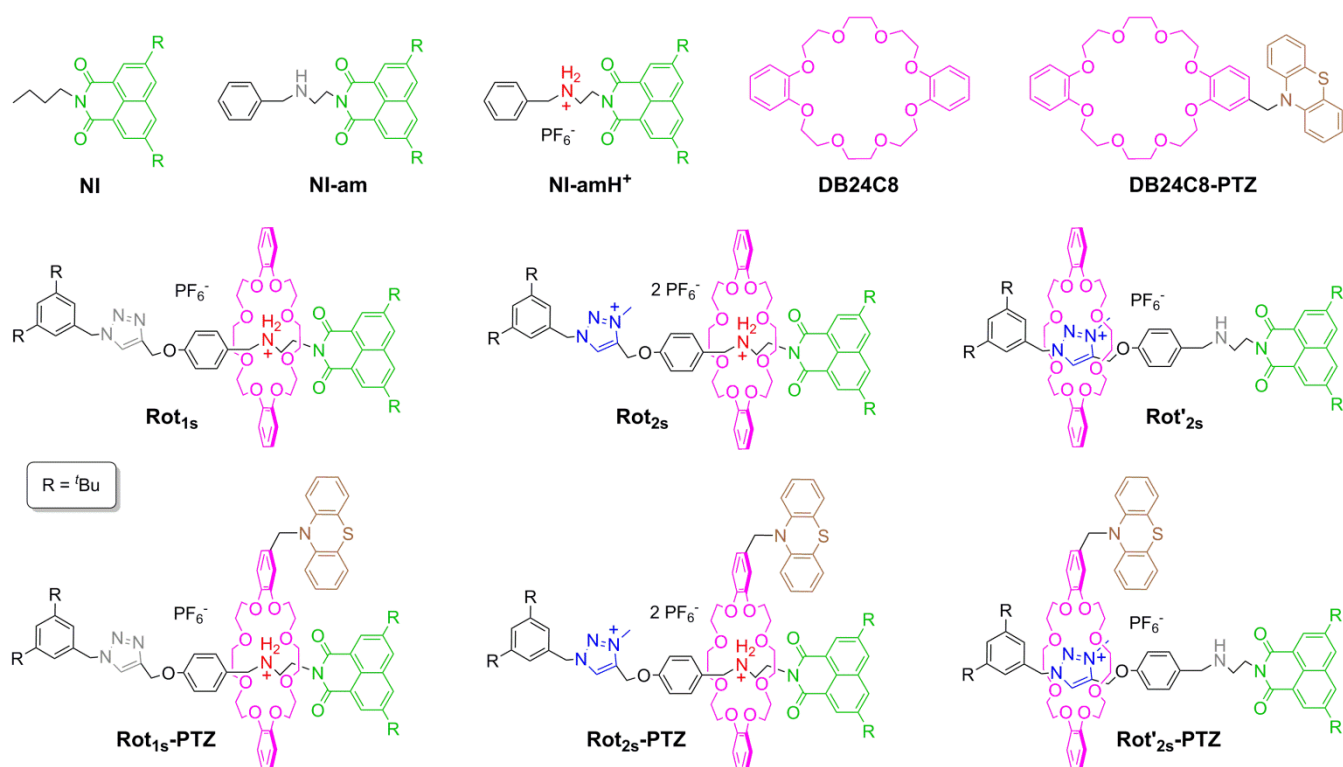
Figure 2. Model compounds, ring components and rotaxanes employed in this work.

NI, **NI-am**, **NI-amH⁺**, **Rot₁ₛ**, **Rot₂ₛ** and **Rot'₂ₛ** were synthesized and fully characterized (^{1}H, ^{13}C, COSY and ROESY NMR spectroscopy, high-resolution mass spectroscopy) in a previous work.[37] The synthesis and characterization (^{1}H and ^{13}C NMR spectroscopy, high-resolution mass spectroscopy) of **DB24C8-PTZ**, **Rot₁ₛ-PTZ**, **Rot₂ₛ-PTZ** and **Rot'₂ₛ-PTZ** are reported in the Supporting Information. The synthesis of the PTZ-containing rotaxanes follows the procedures used for the PTZ-free equivalents. By comparison with **Rot₂ₛ**, the shuttling of the ring by quantitative deprotonation of **Rot₂ₛ-PTZ** to yield **Rot'₂ₛ-PTZ** was unambiguously attested by ^{1}H NMR.

Electrochemistry

The redox properties of NI and PTZ embedded in the rotaxanes **Rot₁ₛ-PTZ** and **Rot₂ₛ-PTZ** were studied by cyclic voltammetry in CH₃CN with 0.1 M Bu₄NPF₆ as the supporting electrolyte (see Figures S20 to S25). The reduction potentials of the NI and PTZ units in these molecules and in pertinent models are listed in Table 1. Both electroactive units in **NI-amH⁺**, **DB24C8-PTZ, Rot₁ₛ-PTZ** and **Rot₂ₛ-PTZ** exhibit a quasi-reversible behavior. The incorporation of NI and PTZ in the rotaxane architecture **Rot₁ₛ-PTZ** affects very moderately the potential values [$\Delta E_{1/2}$(NI) = +50 mV and $\Delta E_{1/2}$(PTZ) = −20 mV], indicating a good electronic insulation of both units from the structural components of the rotaxane. The methylation of the triazolyl moiety in **Rot₁ₛ-**

PTZ to produce the secondary station for **Rot₂ₛ-PTZ** has almost no effect on the measured potentials.

Table 1. Halfwave reduction potentials in V *vs* SCE of the NI and PTZ units. The numbers in parenthesis are the difference between the anodic and cathodic peaks, in mV.[a]

	NI/NI•⁻	PTZ•⁺/PTZ
NI-amH⁺	−1.421 (57)	−
DB24C8-PTZ	−	+0.724 (70)
Rot₁ₛ-PTZ	−1.371 (55)	+0.742 (66)
Rot₂ₛ-PTZ	−1.391 (61)	+0.752 (64)

[a] In CH₃CN, 0.1 M Bu₄NPF₆. For more details see SI.

Absorption and luminescence properties

The electronic absorption spectra were measured in CH₃CN. For all the compounds (except **DB24C8-PTZ**), a band centered at ca. 350 nm with $\varepsilon \approx$ 14000 mol⁻¹.L.cm⁻¹ typical of the NI chromophore is observed.[38-41] In all the rotaxanes, the absorption band of the **DB24C8** macrocycle (λ_{max} = 275 nm) is also detected. For the three PTZ-containing rotaxanes, an overlap of the absorption bands due to the PTZ (maximum at 310 nm) and NI units is observed until ca. 350 nm; for longer

wavelengths the absorption due to PTZ becomes negligible. Interestingly, the NI absorption band in all the protonated rotaxanes has a 2 nm bathochromic shift compared to the band in **NI-amH⁺** (see Figure 1 for a comparison between **NI-amH⁺**, **Rot₁ₛ** and **Rot₁ₛ-PTZ**). Previous studies on NI-containing chromophores pointed out that the maximum of this absorption band is sensitive to the presence of a hydrogen bond donor in the medium.[32, 33, 42] In our case, this shift is attributed to the fact that in **NI-amH⁺** an intramolecular hydrogen bond can be established between the ammonium unit and a carbonyl group of the naphthalimide in the ground state, while in the protonated rotaxanes the ammonium is engaged in a stronger interaction with the crown ether. When excited in the NI absorption band (325 nm), all the compounds exhibit an emission band centered at ca. 390 nm (Figures 3 and S26 to S34). The excitation spectra of the rotaxanes for the emission centered on the NI unit are not entirely superimposable with the corresponding absorption spectra. In particular, the absorption band of **DB24C8** centered at 275 nm is absent in the excitation spectra (with the exception of **Rot₁ₛ** where the band is partially recovered, Figures S26 to S34), indicating the absence of energy transfer from the crown ether to the NI chromophore in the rotaxanes.
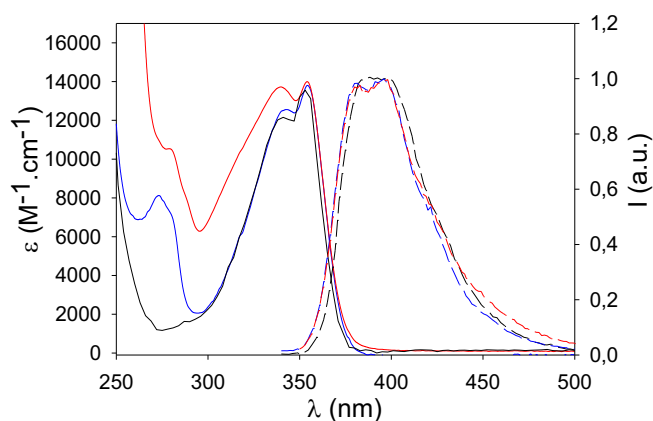
Figure 3. Absorption (—) and emission (– – –) spectra of **NI-amH⁺** (black), **Rot₁ₛ** (blue) and **Rot₁ₛ-PTZ** (red) in CH₃CN (300 K, λ_{exc} = 325 nm) (absorption, excitation and emission spectra of all the explored compounds can be found in the SI, Figures S26-S35).

The fluorescence quantum yields were measured in aerated CH₃CN at 298 K (Table 2). The low quantum yields of fluorescence of the NI chromophore in all the protonated rotaxanes, compared with the naphthalimide models **NI** and **NI-amH⁺**, suggest that the luminescence is strongly quenched by the presence of the DB24C8 ring (with or without functionalization by PTZ). Moreover, the deprotonation of the ammonium also leads to a strong quenching of the fluorescence in **NI-am**, **Rot'₂ₛ** and **Rot'₂ₛ-PTZ**.

Lifetimes were measured both in the ns range with a time-correlated single-photon counting (TCSPC) apparatus (time resolution: 100 ps, see Figures S36 to S45) and in the ps time regime with a streak camera apparatus and a femtosecond oscillator as excitation source (time resolution: 1 ps).

In the ns scale, fluorescence lifetimes of 1.53 ns and 2.66 ns are measured for **NI** and **NI-amH⁺**, respectively. With the ultrafast apparatus, a short rise time of ca. 30 ps is detected only for **NI-amH⁺** (Figure S47). The latter can be ascribed to a fast process involving a species that rapidly converts into ¹NI, presumably an excited state proton transfer favored by the presence of the ammonium group. Indeed, the difference in the ns lifetimes of **NI** and **NI-amH⁺** has been previously ascribed to the presence of an intramolecular hydrogen bond between the ammonium unit and a carbonyl group of the naphthalimide, both in the ground and in the excited state.[33]

Differently from **NI** and **NI-amH⁺**, the fluorescence decay of **NI-am** is dominated by a short lifetime of 7 ps, detected with the streak camera apparatus. This lifetime accounts for 95% (as pre-exponential fraction) of the decay, whereas the remaining 5% is fitted by a lifetime of 1800 ps (Figure S48). The latter component, detected also with the TCSPC system (Tables 2 and S2), can be ascribed to the presence of a very small (≤ 5%) amount of **NI-amH⁺**. The quenched lifetime of 7 ps of the NI singlet accounts for the very low emission quantum yield measured for **NI-am** (< 0.1 %, Table 2).

The presence of multiple emission decays for **Rot₁ₛ** and **Rot₂ₛ** was discussed in a previous work.[37] The longer lifetime in the two-station rotaxane **Rot₂ₛ** was ascribed to the presence of the minor (ca. 0.03 %) co-conformational isomer in which the DB24C8 ring is encircling the triazolium station instead of the ammonium station. Note that this longer component is also found for **Rot₂ₛ-PTZ**. The ultra-fast analysis confirmed the multi-exponential nature of the fluorescence decay of the two rotaxanes, and evidenced a short component on the order of 2 ps and 6 ps for **Rot₁ₛ** and **Rot₂ₛ**, respectively (Figure S49). The decays can be reasonably fitted by a tri-exponential function, with τ_2 and τ_3 of the order of 200 ps and 600-700 ps, matching the values obtained with the TCSPC analysis (Table 2). It is evident that for **Rot₂ₛ** a longer component exceeding the time scale of the streak camera is also present (Figure S49b).

For **Rot'₂ₛ**, the streak camera analysis shows that the decay is dominated by a 10 ps component (80% as pre-exponential fraction) followed by components of ca. 100 and 600 ps, and by a longer tail extending over the time scale of the apparatus (Figure S50), well matching with the distribution detected in the TCSPC analysis.

The PTZ containing rotaxanes **Rot₁ₛ-PTZ** and **Rot₂ₛ-PTZ** show TCSPC distributions similar to their parents **Rot₁ₛ** and **Rot₂ₛ** (Table 2). The ps analysis confirmed lifetimes in the order of 200 ps and 550 ps for both rotaxanes but also evidenced a prompt decay close to the time resolution of the system (1 ps, not processable for this reason) (Figure S51). In **Rot'₂ₛ-PTZ** the decay is dominated by a short lifetime of 5 ps (Figure S52) with two residual lifetimes of ca. 200 ps and > 600 ps that could be better detected on the ns range (Table 2).

Overall, the detailed fluorescence analysis evidenced that in all rotaxanes a fast process (1-10 ps) is responsible for the quenching of the NI chromophore. The detected longer lifetime components can be ascribed to the decay of the NI excited singlet in different conformations of the ring around the ammonium site (*vide infra*). At this stage, the influence of the

functionalization of DB24C8 by the donor unit PTZ and of the position of the ring on the axle, as key structural factors in the quenching of the luminescence of NI, cannot be unambiguously demonstrated. Further information and evidences regarding the quenching mechanisms in the different compounds were obtained by transient absorption spectroscopy.

Table 2. Fluorescence data (quantum yields Φ, lifetimes τ_i) for some selected compounds in aerated CH_3CN at 298 K.

	Φ / %	τ_1[a]	τ_2[b]	τ_3[b]	τ_4[b]
			τ_i / ps		
NI	18.4 ± 1	–	–	–	1530
NI-amH$^+$	20.2 ± 1.2	–	–	–	2660
NI-am	< 0.1	7	[c]	–	1750
Rot$_{1s}$	1.0 ± 0.1	2	190	620	–
Rot$_{2s}$	1.8 ± 0.2	6	220	760	2620
Rot'$_{2s}$	~ 0.1	10	140	610	2080
Rot$_{1s}$-PTZ	0.6 ± 0.1	~ 1	170	580	–
Rot$_{2s}$-PTZ	1.3 ± 0.1	~ 1	170	540	2430
Rot'$_{2s}$-PTZ	0.3 ± 0.1	5	270	–	1720

[a]   From streak-camera analysis (time resolution: 1 ps); λ_{exc} = 350 nm; [b] from TCSPC analysis (time resolution: 100 ps); λ_{exc} = 340 nm, λ_{em} = 415 nm. The pre-exponential factors measured by TCSPC analysis are given in SI. All the fluorescence intensity decays are shown in the SI; [c]   a decay component shorter than the time resolution of the TCSPC apparatus is detected (see Figure S38).

Transient absorption spectroscopy

Pump-and-probe experiments with femtosecond resolution were carried out on all compounds in aerated CH_3CN. Excitation at 350 nm was performed in order to achieve almost exclusive excitation of the NI component also in the PTZ containing rotaxanes.

Model compound **NI** shows an end-of–pulse spectrum with maximum at 481 nm and a weak and broad absorption in the 700-800 nm region, which evolves into a species absorbing at 474 nm (Figure S53). The observed process is identified as the $S_1 \rightarrow T_1$ intersystem crossing of the NI chromophore, confirmed by the lifetime of 1500 ps measured over the whole spectral range (Figure S53b). The decay shows a second component, almost constant in the time range of the experiment, due to the formed triplet. The observed transient spectra are in reasonable agreement with those reported for singlet and triplet excited states of NI chromophores.[39, 40, 43-45] Very similar features are observed for **NI-amH$^+$**, where the spectral evolution is consistent with intersystem crossing (Figure S54a). The absorption maxima of the singlet and triplet excited states in this case are 474 nm and 477 nm, respectively. The time evolution is dominated by a decay of 2400 ps, consistent with the fluorescence lifetime[46] but, at a difference with **NI**, a prompt decay of 20 ps is detected in the 480-550 nm region (Figure S54b). This behavior is in agreement with the luminescence outcome and the short-lived

species can be ascribed to a protonated form of the NI chromophore.

A completely different scenario is observed for model **NI-am**. The end-of-pulse signal, ascribable to the NI singlet, shows a bi-exponential decay dominated by a short component of the order of 7 ps, followed by a longer decay of ca. 1600 ps accounting for about 1 % of the total band intensity (Figure S55). In the 470-480 nm region a further slow signal rise is detected (Figure S55b). The data can be interpreted on the basis of a fast quenching of ^{1}NI due to an electron transfer process from the amine group. The spectral features of the naphthalimide anion, to be expected in the 700-800 nm region (see below), cannot be identified,[47] most likely because of an ultrafast (≤ 300 fs) charge-recombination process. The second minor decay component (1500 ps) is consistent with the longer lifetime observed from luminescence measurements and it evolves in the population of the NI triplet state, as confirmed by the signal rise at 470-480 nm.

The two DB24C8-containing rotaxanes with the ring encircling the ammonium station, **Rot$_{1s}$** and **Rot$_{2s}$**, show a similar behavior. The time evolution of ΔA in the 450-540 nm region is satisfactory fitted by three exponentials, with lifetimes of 2.5 ps, 100 ps and 620 ps for **Rot$_{1s}$** and 5 ps, 250 ps and 740 ps for **Rot$_{2s}$** (Figures S56 and S57). Two bands, at ca. 735 nm and 790 nm, form with a rise time consistent with the shortest decay observed in the 450-540 nm region and then decay in 740 ps for **Rot$_{1s}$** and 820 ps for **Rot$_{2s}$**. These bands can be safely ascribed to the naphthalimide anion, since the spectrum of **NI-am** obtained by spectroelectrochemistry (Figure S46) clearly evidences their presence together with an intense peak at ca. 420 nm, usually reported for NI anions.[31, 48-50] The radical cation of 1,2-dimethoxybenzene, that can be considered as a model for the DB24C8 ring, has been reported to show absorption features at ca. 400-430 nm, a region outside the spectral range of our analysis.[51-53] The presence of two longer components in the region of absorption of the singlet state can be ascribed to different conformations of the rotaxane, where the distance between the dioxybenzene moieties of the crown ether and the NI unit is larger, thus hindering the electron transfer process. The observed lifetimes are in good agreement with those measured for the luminescence decays (Table 2) and can be tentatively assigned to two different conformations of the ring around the ammonium site, characterized by the presence of intramolecular hydrogen bonds in the ground state[54-56] and/or proton-transfer processes in the excited-state. On long time scales, a weak signal at 478 nm, attributable to ^{3}NI, is detected (Figures S56a and S57a).

When the ring resides on the tria$^+$ station, its interaction with the NI unit is negligible. Indeed, the transient absorption behavior of **Rot'$_{2s}$** is very similar to that of **NI-am**. The signal evolves mainly with a short decay of the order of 10 ps, followed by a longer one of ca. 1000 ps (accounting for ca. 20 %, Figure S58). In the 470-480 nm region a further slow signal rise is detected. The main decay can be ascribed to a PET process from the amine group to the NI chromophore.

a)

b)
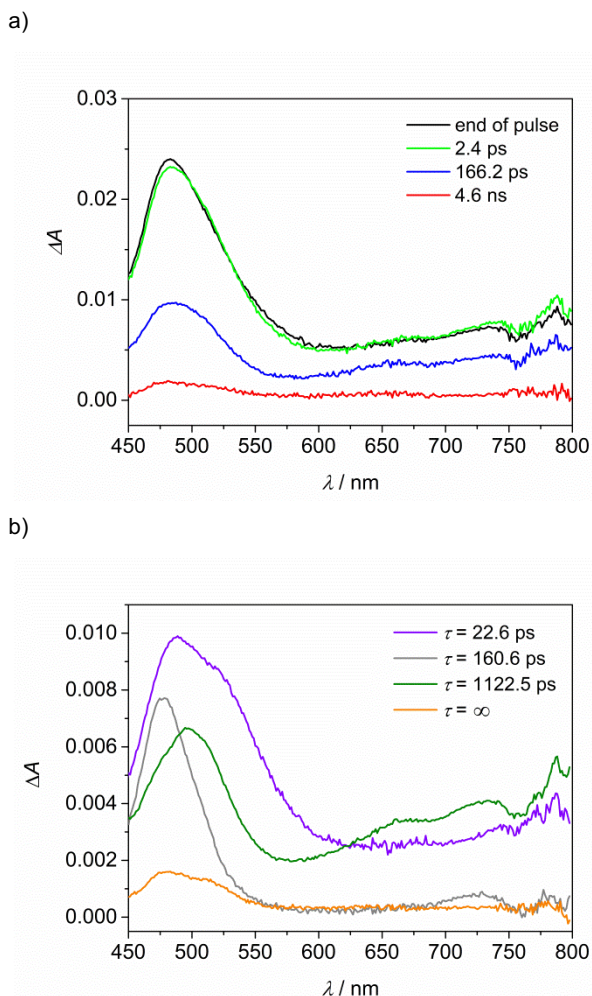
Figure 4. a) Transient absorption spectra of **Rot$_{1s}$-PTZ** in CH$_3$CN measured at the end of pulse and at various delays. b) Spectral distribution of the amplitudes of the calculated lifetimes (indicated in the legend) from global fit analysis of the transient absorption matrix (obtained with four principal components and three expected lifetimes, plus an infinite lifetime). λ_{exc}= 350 nm (A_{350} = 0.2, 2 mm optical path).
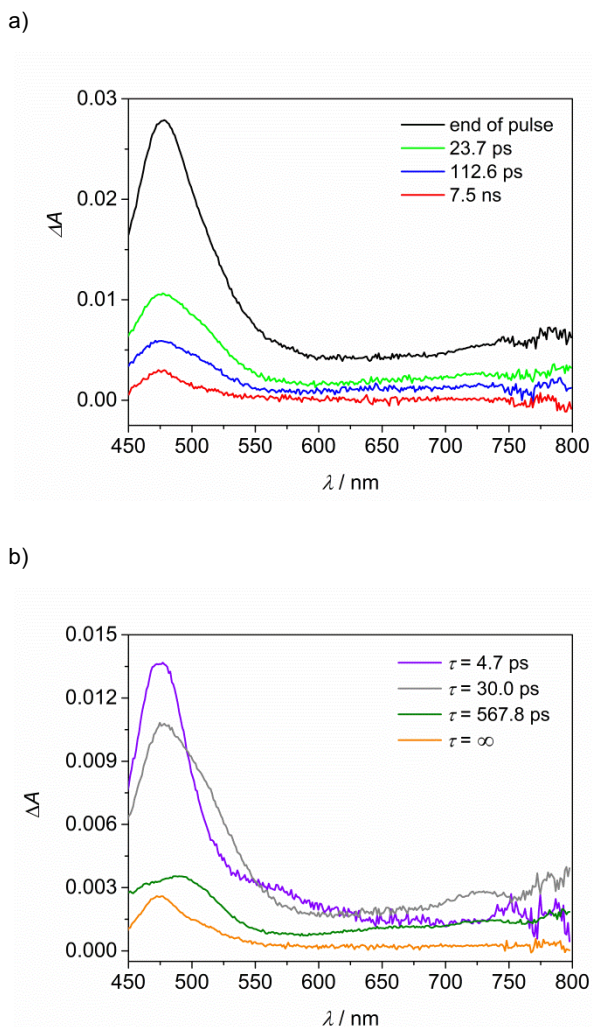
Transient absorption analysis of the PTZ containing rotaxanes evidences additional features, with a similar behavior for **Rot$_{1s}$-PTZ** and **Rot$_{2s}$-PTZ**. Figure 4 shows the time evolution of the transient absorption of **Rot$_{1s}$-PTZ**. In the 450-500 nm region multi-exponential decays are detected, with an initial short component of ca. 1 ps. At 780-790 nm a short rise in the order of 1 ps is detected and the 500-800 nm region is characterized by a bi-exponential decay with lifetimes of ca. 25 ps and 1000 ps with equal weight (Figure 4a and S59 for time evolution). To get further insights in the comprehension of the transient data, a global fit analysis has been performed. Figure 4b shows the spectral distribution of the amplitudes of the calculated lifetimes. A lifetime of 160 ps has a spectral distribution typical of ^{1}NI and can be associated to the decay of a NI unit not quenched by PET processes but affected by the environment (it corresponds to a detected luminescence lifetime of 170 ps). The spectral distribution of the infinite lifetime is consistent with a triplet

excited state which can be populated by the unquenched NI singlet. The other two spectra, associated with lifetimes of 23 ps and 1100 ps, show features ascribable to a PTZ$^+$-NI$^-$ state: the bands in the 700-800 nm identify the naphthalimide anion and the bands in the 500-550 nm region are ascribable to the phenothiazine cation, whose absorption is reported at 520 nm.[31, 35, 57] Interestingly, two different lifetimes are found for the decay of the CS state. A plausible explanation is the existence of two different conformations of the ring on the axle governing the distance between the units. Due to the overlap of the signals, we have no clear evidence for the formation of the CS state crown$^+$-NI$^-$ prior to formation of PTZ$^+$-NI$^-$.

Very similar transient features are observed for **Rot$_{2s}$-PTZ** (Figure S60). Creation of the charge separated states occurs within the formation of the signal, with a kinetic faster or on the order of the instrumental time resolution (300 fs). From global analysis, three lifetimes (and an infinite component) were identified (Figure S60b). One component has a lifetime of 204 ps and is associated with an unquenched ^{1}NI; it corresponds to the main component of the luminescence decay (170 ps, Table 2). Two lifetimes of 24 ps and 1090 ps are distributed with features ascribable to a PTZ$^+$-NI$^-$ CS state. The long (infinite) lifetime can be associated with ^{3}NI.

The behavior of **Rot'$_{2s}$-PTZ** is more peculiar. At 470 nm a multi-exponential decay is detected, dominated by a first component of ca. 5 ps (Figure 5a and S61). This short lifetime can be attributed to the quenching of the NI singlet by the amine group through a PET process, in a conformation where the PTZ unit is not in close proximity to the NI chromophore. Weak features of the PTZ$^+$-NI$^-$ CS state are observed, and their formation occurs within the formation of the signal. The decay in the CS spectral region (500-800 nm) is described by a bi-exponential function with lifetimes of ca. 25 ps and 570 ps, with 70 % and 30 % in weight, respectively. From a global analysis, three lifetimes (and an infinite lifetime component) with the spectral distribution shown in Figure 5b are identified. The dominating component in the 450-500 nm region is a short lifetime of ca. 5 ps, associated with ^{1}NI quenched by the amine group. Two lifetimes of 30 ps and 570 ps are distributed with features ascribed to the PTZ$^+$-NI$^-$ state. For similarity with the other rotaxanes, they are associated to two different conformations of the ring. The infinite lifetime is associated with triplet features.

a)

b)

Figure 5. a) Transient absorption spectra of **Rot'$_{2s}$-PTZ** in CH$_3$CN measured at the end of pulse and at various delays. b) Spectral distribution of the amplitudes of the calculated lifetimes (indicated in the legend) from global fit analysis of the transient absorption matrix (obtained with four principal components and three expected lifetimes, plus an infinite lifetime). λ_{exc}= 350 nm (A_{350} = 0.2, 2 mm optical path).

Overall, the transient absorption data evidence excited state deactivation kinetics in good agreement with those measured in the fluorescence analysis, shining light on the nature of the electron transfer processes involved in the different systems.

The closeness of the deprotonated amine group is responsible for the fast quenching of the NI unit in **NI-am**, **Rot'$_{2s}$** and partially in **Rot'$_{2s}$-PTZ** (the latter being the rotaxanes with the ring shifted on the tria$^+$ station) through a PET process from the amine group to NI. In **Rot$_{1s}$** and **Rot$_{2s}$**, where the ring encircles the amH$^+$ station and is in close proximity of the NI unit, the identified PET reaction is from the DB24C8 ring to NI. Finally, in the PTZ containing rotaxanes **Rot$_{1s}$-PTZ** and **Rot$_{2s}$-PTZ**, the PET process from the PTZ unit to the NI chromophore appears to be predominant. In **Rot'$_{2s}$-PTZ**, both am→NI and PTZ→NI electron transfer processes are detected, probably due to the presence of conformations where the PTZ unit is pointing either away or

towards to the NI acceptor. It can be noticed that the kinetics of the various processes are different: the am→NI PET process occurs in a time scale of 5-10 ps, the crown→NI PET is slightly faster, with time constants of 2-5 ps, whereas the PTZ→NI reaction is very fast, with τ below or around 1 ps. The latter, indeed, is the reaction with the highest driving force (figure 6).

Conclusions

Six rotaxanes comprising an electron-donor macrocycle and bearing an electron-acceptor naphthalimide chromophore (NI) at one extremity of the axle have been synthesized, characterized and submitted to a comprehensive photophysical study. These rotaxanes were designed to evaluate several factors which can govern the events following the photogeneration of the NI singlet, namely: i) the presence of a secondary station for the ring along the axle; ii) the flexibility of the components and the presence of several (co-)conformations; iii) the functionalization of the DB24C8 ring with a phenothiazine (PTZ) unit; iv) the position of the ring along the axle.

The comparison of two dyads containing one primary ammonium station and either an innocent triazolyl moiety (**Rot$_{1s}$**) or a triazolium unit that can act as a secondary station for the ring (**Rot$_{2s}$**) rules out a significant role of the secondary station in the photophysical behavior, and confirms that the macrocycle is surrounding the amH$^+$ site in the vast majority of the **Rot$_{2s}$** species. [37] In both cases, the multiexponential decay of the NI singlet excited state indicates the presence of different conformations in which the excited NI unit either generates the charge separated state crown$^+$-NI$^-$, which recombine with similar lifetimes (ca. 800 ps) in the two rotaxanes, or is not quenched by PET processes. We hypothesize that intramolecular hydrogen bonding and/or excited-state proton transfer processes between the ammonium center and the NI unit may be at the basis of the latter behavior.

In the PTZ-functionalized rotaxanes **Rot$_{1s}$-PTZ** and **Rot$_{2s}$-PTZ**, photoexcitation of NI produces the charge separated state PTZ$^+$-NI$^-$ within 1 ps, while there is no evidence for the participation of the crown ether as an electron donor in PET processes. The charge recombination is characterized in both cases by two very different lifetimes (ca. 25 ps and 1 ns), which can be attributed to the presence of two distinct conformations in the CS state. Rotaxanes wherein the NI singlet excited state is not quenched by PET are also observed, as discussed for the parent **Rot$_{1s}$** and **Rot$_{2s}$**. Finally, the study of the two deprotonated rotaxanes **Rot'$_{2s}$** and **Rot'$_{2s}$-PTZ**, in which the ring interacts with the triazolium station and a free amine is located close to the NI chromophore, highlights the strong involvement of the amine as an electron donor moiety in PET. Indeed, in **Rot'$_{2s}$**, the NI quenching is dominated by PET from the free amine, while in **Rot'$_{2s}$-PTZ** an electron transfer process from the PTZ unit to the excited ^{1}NI level is also detected.
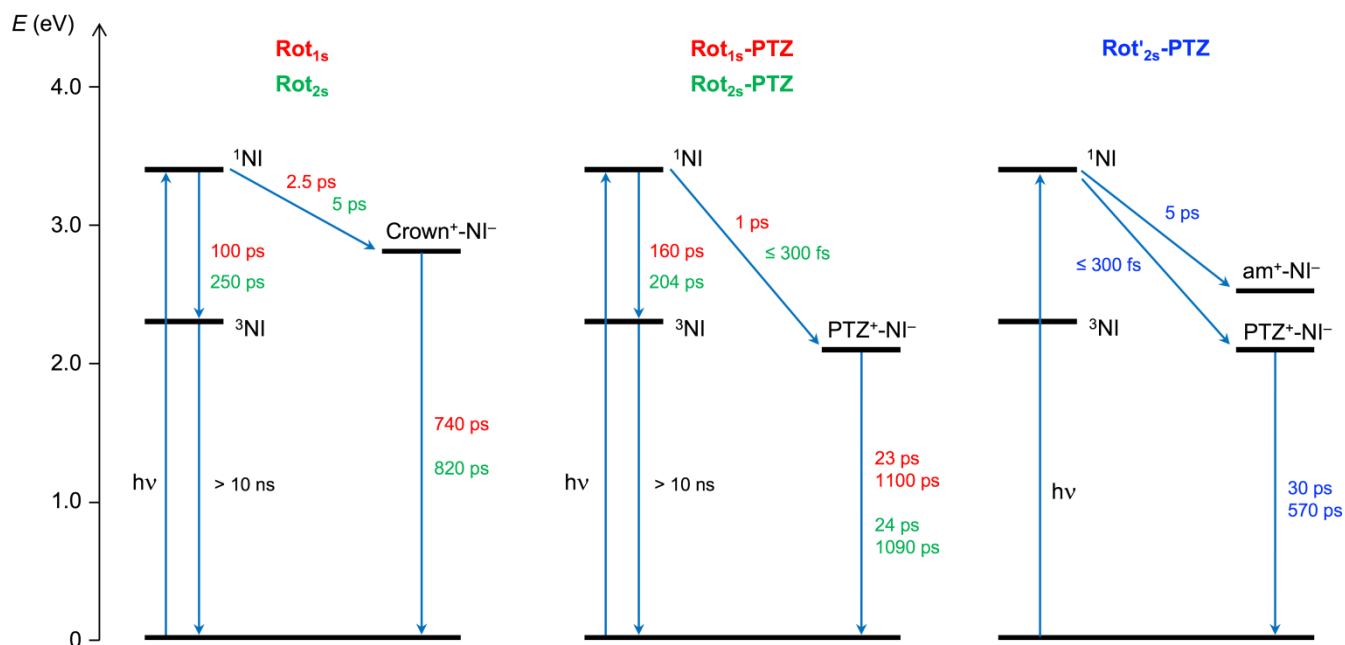
Figure 6. Simplified energy-level diagram with a schematic representation of the main photophysical processes that occur in the different rotaxanes. The different arrows departing from the same ^{1}NI excited state denote processes that occur in different conformations of the rotaxane and are not comptetitive processes that can occur in the same conformation. The reported lifetimes are those measured by transient absorption spectroscopy (from global analysis, in particular, when performed; see the text). The energy values of the NI-localized singlet and triplet excited states have been taken from the literature,[31] while those of the charge-separated states have been estimated from redox potentials determined in this work or reported in the literature. [14]

In summary, this study clearly shows that in rather simple rotaxane-based dyads the intra- and inter-component mobility leads to a complex situation in which multiple photoinduced pathways are active. Chemical switching – namely, deprotonation/protonation – affects the photophysical behavior of the two-station rotaxanes, in a way which is not exclusively related to the donor-acceptor distance change caused by the modified ring-axle arrangement. These findings suggest that rotaxanes with more rigid components are needed in order to exploit stimuli-controlled ring shuttling for modulating intercomponent PET reactions. On the other hand, our work highlights that flexible multichromophoric rotaxanes can enable the occurrence of through-space electron transfer in spatially organized chromophores and can provide new challenges for the experimental investigation of complex dynamic processes, thereby revealing useful to probe the functional sophistication of natural architectures.

Experimental Section

Synthetic procedures, characterization of the compounds, additional spectroscopic and electrochemical data are available in the supporting information. The following file is available free of charge.

Acknowledgements

[1]   J. Deisenhofer, O. Epp, K. Miki, R. Huber, H. Michel, *Nature* **1985**, *318*, 618−624.

[2]   C. C. Moser, J. M. Keske, K. Warncke, R. S. Farid, P. L. Dutton, *Nature* **1992**, *355*, 796−802.

[3]   C.J. Bruns, J.F. Stoddart, *The Nature of the Mechanical Bond - From Molecules to Machines*, Wiley, Hoboken, **2017**.

[4]   M.-J. Blanco, M. C. Jiménez, J.-C. Chambron, V. Heitz, M. Linke, J.-P. Sauvage, *Chem. Soc. Rev.* **1999**, *28*, 293−305.

[5]   M. Linke, J.-C. Chambron, V. Heitz, J.-P. Sauvage, *J. Am. Chem. Soc.* **1997**, *119*, 11329−11330.

[6]   M. Andersson, M. Linke, J.-C. Chambron, J. Davidsson, V. Heitz, J.-P. Sauvage, L. Hammarström, *J. Am. Chem. Soc.* **2000**, *122*, 3526−3527.

[7]   M. Linke, J.-C. Chambron, V. Heitz, J.-P. Sauvage, S. Encinas, F. Barigelletti, L. Flamigni, *J. Am. Chem. Soc.* **2000**, *122*, 11834−11844.

[8]   N. Armaroli, F. Diederich, C. O. Dietrich-Buchecker, L. Flamigni, G. Marconi, J.-F. Nierengarten, J.-P. Sauvage, *Chem. Eur. J.* **1998**, *4*, 406−416.

[9]   N. Watanabe, N. Kihara, Y. Furusho, T. Takata, Y. Araki, O. Ito, *Angew. Chem. Int. Ed.* **2003**, *42*, 681−683.

[10]   E. Jakob, A. Berg, R. Rubin, H. Levanon, K. Li, D. I. Schuster, *J. Phys. Chem. A* **2009**, *113*, 5846−5854.

[11] J. D. Megiatto Jr, D. I. Schuster, G. de Miguel, S. Wolfrum, D. M. Guldi, *Chem. Mater.*, **2012**, *24*, 2472–2485.

[12] S. V. Kirner, C. Henkel, D. M. Guldi, J. D. Megiatto Jr, D. I. Schuster, *Chem. Sci.* **2015**, *6*, 7293−7304.

[13] A. Mateo-Alonso, C. Ehli, G. M. A. Rahman, D. M. Guldi, G. Fioravanti, M. Marcaccio, F. Paolucci, M. Prato, *Angew. Chem. Int. Ed.* **2007**, *46*, 3521–3525.

[14] P. R. Ashton, R. Ballardini, V. Balzani, I. Baxter, A. Credi, M. C. T. Fyfe, M. T. Gandolfi, M. Gómez-López, M.-V. Martínez-Díaz, A. Piersanti, N. Spencer, J. F. Stoddart, M. Venturi, A. J. P. White, D. J. Williams, *J. Am. Chem. Soc.* **1998**, *120*, 11932−11942.

[15] P. Franchi, V. Bleve, E. Mezzina, C. Schäfer, G. Ragazzon, M. Albertini, D. Carbonera, A. Credi, M. Di Valentin, M. Lucarini, *Chem. Eur. J.* **2016**, *22*, 8745–8750.

[16] P. R. Ashton, R. Ballardini, V. Balzani, M. C. T. Fyfe, M. T. Gandolfi, M.-V. Martínez-Díaz, M. Morosini, C. Schiavo, K. Shibata, J. F. Stoddart, A. J. P. White, D. J. Williams, *Chem. Eur. J.* **1998**, *4*, 2332–2341.

[17] P. R. Ashton, I. Baxter, M. C. T. Fyfe, F. M. Raymo, N. Spencer, J. F. Stoddart, A. J. P. White, D. J. Williams, *J. Am. Chem. Soc.* **1998**, *120*, 2297−2307.

[18] S. J. Cantrill, D. A. Fulton, A. M. Heiss, A. R. Pease, J. F. Stoddart, A. J. P. White, D. J. Williams, *Chem. Eur. J.* **2000**, 6, 2274 –2287.

[19] F. Coutrot, E. Busseron, *Chem. Eur. J.* **2008**, *14*, 4784−4787.

[20] F. Coutrot, C. Romuald, E. Busseron, *Org. Lett.* **2008**, *10*, 3741−3744.

[21] E. Busseron, C. Romuald, F. Coutrot, *Chem. Eur. J.* **2010**, *16*, 10062−10073.

[22] C. Romuald, A. Arda, C. Clavel, J. Jimenez-Barbero, F. Coutrot, *Chem. Sci.* **2012**, *3*, 1851−1857.

[23] V. Blanco, A. Carlone, K. D. Hänni, D. A. Leigh, B. A. Lewandowski, *Angew. Chem., Int. Ed.* **2012**, *51*, 5166−5169.

[24] E. Busseron, F. Coutrot, *J. Org. Chem.* **2013**, *78*, 4099−4106.

[25] S. Chao, C. Romuald, K. Fournel-Marotte, C. Clavel, F. Coutrot, *Angew. Chem. Int. Ed.* **2014**, *53*, 6914−6919.

[26] V. Blanco, D. A. Leigh, U. Lewandowska, B. Lewandowski, V. Marcos, *J. Am. Chem. Soc.* **2014**, *136*, 15775−15780.

[27] V. Blanco, D. A. Leigh, V. Marcos, J. A. Morales-Serna, A. L. Nussbaumer, *J. Am. Chem. Soc.* **2014**, *136*, 4905−4908.

[28] F. Coutrot, *Chemistry Open* **2015**, *4*, 556−576.

[29] P. Waelès, B. Riss-Yaw, F. Coutrot, *Chem. Eur. J.* **2016**, *22*, 6837−6845.

[30] S. Corra, C. de Vet, J. Groppi, M. La Rosa, S. Silvi, M. Baroncini, A. Credi, *J. Am. Chem. Soc.* **2019**, *141*, 9129-9133.

[31] D. W. Cho, M. Fujitsuka, A. Sugimoto, U. C. Yoon, P. S. Mariano, T. Majima, *J. Phys. Chem. B* **2006**, *110*, 11062-11068.

[32] D. W. Cho, M. Fujitsuka, U. C. Yoon, T. Majima, *J. Photochem. Photobiol. A: Chem.* **2007**, *190*, 101–109.

[33] D. W. Cho, M. Fujitsuka, U. C. Yoon, T. Majima, *Phys. Chem. Chem. Phys.* **2008**, *10*, 4393–4399.

[34] T. Takada, K. Kawai, M. Fujitsuka, T. Majima, *Proc. Natl. Acad. Sci. U.S.A.* **2004**, *101*, 14002–14006.

[35] P. A. Scattergood, M. Delor, I. V. Sazanovich, O. V. Bouganov, S. A. Tikhomirov, A. S. Stasheuski, A. W. Parker, G. M. Greetham, M. Towrie, E. S. Davies, A. J. H. M. Meijer, J. A. Weinstein, *Dalton Trans.* **2014**, *43*, 17677-17693.

[36] N. Pearce, E. S. Davies, R. Horvath, C. R. Pfeiffer, X.-Z. Sun, W. Lewis, J. McMaster, M. W. George, N. R. Champness, *Phys. Chem. Chem. Phys.* **2018**, *20*, 752–764.

[37] G. Ragazzon, A. Credi, B. Colasson, *Chem. Eur. J.* **2017**, *23*, 2149–2156.

[38] M. S. Alexiou, V. Tychopoulos, S. Ghorbanian, J. H. P. Tyman, R. G. Brown, P. L. Brittain, *J. Chem. Soc. Perkin Trans. 2* **1990**, 837–842.

[39] B. M. Aveline, S. Matsugo, R. W. Redmond, *J. Am. Chem. Soc.* **1997**, *119*, 11785–11795.

[40] P. Kucheryavy, G. Li, S. Vyas, C. Hadad, K. D. Glusac, *J. Phys. Chem. A* **2009**, *113, 23*, 6453–6461.

[41] B. Ventura, A. Bertocco, D. Braga, L. Catalano, S. d'Agostino, F. Grepioni, P. Taddei, *J. Phys. Chem. C* **2014**, *118*, 18646–18658.

[42] V. Wintgens, P. Valat, J. Kossanyi, L. Biczók, A. Demeter, T. Bérces, *J. Chem. Soc. Faraday Trans.* **1994**, *90*, 411–421.

[43] A. Samanta, G. Saroja, *J. Photochem. Photobiol. A: Chem.* **1994**, *84*, 19–26.

[44] D. W. Cho, D. W. Cho, H. J. Park, U. C. Yoon , M. H. Lee, C. Im, *J. Photochem. and Photobiol. A: Chem.* **2012**, *246*, 23–28.

[45] A. Samanta, B. Ramachandram, G. Saroja, *J. Photochem. and Photobiol. A: Chem.* **1996**, *101*, 29–32.

[46] This value is slightly underestimated because it is at the limit of the maximum lifetime measurable by the apparatus, ca. 2.0 ns.

[47] A. D. Johnson, K. A. Paterson, J. C. Spiteri, S. A. Denisov, G. Jonusauskas, A. Tron, N. D. McClenaghan, D. C. Magri, *New J. Chem.* **2016**, *40*, 9917–9922.

[48] D. Gosztola, M. P. Niemczyk, W. Svec, A. S. Lukas, M. R. Wasielewski, *J. Phys. Chem. A* **2000**, *104*, 6545–6551.

[49] J. E. Rogers, L. A. Kelly, *J. Am. Chem. Soc.* **1999**, *121*, 3854-3861.

[50] S. Ghosh, S. Biswas, M. Mondal, S. Basu, *J. of Luminescence* **2014**, *145*, 410–419.

[51] C. Sieiro, P. Calle, N. Lorenzo, *J. Mol. Structure (Theochem)* **1998**, *433*, 329–338.

[52] Y. Yagci, W. Schanbel, A. Wilbert, J. Bendig, *J. Chem. Soc. Faraday Trans.* **1994**, *90*, 287–291.

[53] T. A. Gadosy, D. Shukla, L. J. Johnston, *J. Phys. Chem. A* **1999**, *103*, 8834–8839.

[54] K. Matsubayashi, Y. Kubo, *J. Org. Chem.* **2008**, *73*, 4915–4919.

[55] K. Matsubayashi, C. Kajimura, H. Shiratori, Y. Kubo, T. Yoshihara, S. Tobita, *Bull. Chem. Soc. Jap.* **2010**, *83*, 1067–1073.

[56] D. P. Yang, H. Li, Y. F. Liu, *J. Chin. Chem. Soc.* **2013**, *60*, 267–274.

[57] M. Barra, R. W. Redmond, M. T. Allen, G. S. Calabrese, R. Sinta, J. C. Scalano, Photochemistry of Phenothiazine Sensitizers in Poly(methylmethacrylate) Films. *Macromolecules* **1991**, *24*, 4972–4977.

FULL PAPER

Electron traffic: multiple light-induced electron-transfer processes are enabled by mechanically interlocking molecular components that comprise chromophoric, electron-donor and electron-acceptor units.
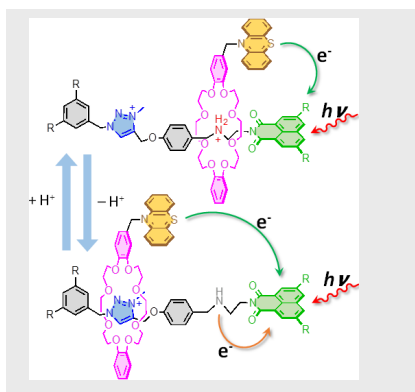
Benoit Colasson, Alberto Credi* and Barbara Ventura**

Page No. – Page No.

Photoinduced Electron Transfer Involving a Naphthalimide Chromophore in Switchable and Flexible [2]Rotaxanes